Palestine Journal of Mathematics

Vol. 11(2)(2022) , 617–629

Image deblurring by periodic and Neumann boundary conditions in a wavelet domain

A. Padmanabha Reddy and K. Riyajuddin

Communicated by V. Lokesha

MSC 2020 Classifications: Primary 15A18, 65T60; Secondary 68U10.

Keywords and phrases: Singular value decomposition, Haar wavelet, Image deblurring.

Author K. Riyajuddin, Research Scholar, is thankful to Govt. of Karnataka Directorate of Minorities (GOKDOM), India, for providing minority fellowship to carry out the present research work.

Abstract The blur removal is an important problem in signal and image processing applications for computing faithful representation of an original scene from a blurred noisy image. The specific structure of the blurring matrices depends on boundary conditions. When zero boundary conditions are used, then coefficient matrix is a Toeplitz matrix. If the periodic boundary conditions are used, then coefficient matrices become circulant matrices. The blurring matrices obtained by using Neumann boundary conditions are Toeplitz-plus-Hankel matrices. In this paper, we formulate deblurring problem by using Truncated Singular Value Decomposition (TSVD) and Discrete Wavelet Transform (DWT) method and estimating regularization parameter when generalized cross-validation is used. Finally, we demonstrate the efficiency of our approximation in a DWT method by numerical experiments.

1 Introduction

In signal and image processing the problem of deblurring is to recover f from the blurred function g. This basic problem appears in many forms in signal and image processing [1, 2, 3]. Image restoration is the process of reconstructing an image of an unknown scene from an observed image but blurred image, which is often modeled as

$$g = Kf + \eta \tag{1.1}$$

where f is a vector representing the true image, vector η represents additive noise and g stands for the blurred noisy image. K is an blurring matrix constructed from a point spread function (PSF), which specifies how points in the image are distorted. A blur is said to be spatially invariant if every position in the image domain gets blurred by the same PSF and spatially variant if different positions are governed by different PSFs. The spatially invariant blur occurs most frequently in applications [3]. Because the blurring model is a convolution, g is not only determined by f, but also the values of f outside the domain where g is defined. Thus in solving f from g, we need some assumptions on the data outside the boundary, called boundary conditions. The structure of the blurring matrix K depends on the boundary conditions [4].

The zero (Dirichlet) boundary condition assumes that the values of f outside the domain of consideration are zero. The resulting blurring matrix is Toeplitz in the one-dimensional case and a block-Toeplitz-Toeplitz-block (two-level Toeplitz) in the two-dimensional case [5]. If a signal or an image has boundaries, and if the true signal or image is not close to zero at the boundaries, the zero boundary conditions are introducing an artificial discontinuity, which leads to ringing effects in the reconstructed image. Also, these matrices are widely known to be computationally expensive to invert, especially in the two-dimensional case [5]. .

One possible way to drastically alleviate the computational cost is to impose the periodic boundary conditions; i.e., data outside the domain of consideration are periodically extended. This results in a blurring matrix which is a circulant matrix in the one-dimensional case and block-circulant-circulant-block matrix in the two-dimensional case [1]. The ciculant matrices can always be diagonalized by discrete Fourier matrices and thus their inverses can easily found by using the fast Fourier transforms; see [1]. However ringing effects will appear unless f is close to periodic, and that is not common in practice. Several image restoration methods have used to solve image deblurring problem [4, 6, 7, 8, 17, 18]. Ng et al. [4] proposed the Neumann boundary conditions, which assumes that the data outside the domain as a reflection of data inside. This choice leads to fast algorithms for solving (1.1) because the blurring matrix results to a special class of Toeplitz-plus-Hankel matrices in one-dimensional case and block Toeplitz-plus-Hankel matrices with Toeplitz-plus-Hankel blocks in two-dimensional case which can be diagonalized by discrete cosine transform matrix provided that the blurring function is symmetric. Also their inverses can be found by using fast cosine transforms (FCTs) which is faster than that of those matrices obtained from either zero or the periodic boundary conditions. Cheng et al. [17] proposed blind image deblurring via hybrid deep priors modeling (HDPM) to simulate the propagation of sharp latent image in kernel estimation and final deconvolution. Zhang et al. [18] proposed a novel network for joint image deblurring and super-resolution that handles both tasks jointly and boosts the super-resolution performance from blurry input greatly.

In this paper we consider using TSVD for image restoration problem in a wavelet domain. The TSVD analysis that suggest the TSVD as one method for dealing with the inverted noise to solve the image deblurring problem. We also present regularization parameter to achieve stability for large ill-conditioning of the blurring matrices. In addition, numerical examples are given to illustrate the performance of the proposed TSVD-based regularization algorithm.

The outline of the paper is as follows. Section 2 introduces the three different boundary conditions. Section 3 introduces the concepts TSVD and DWT briefly. In Section 4, proposed algorithm steps in detail. Section 5 presents numerical results to demonstrate the efficiency of the proposed algorithm. Concluding remarks are given in section 6.

2 The boundary conditions

For simplicity, we first consider with the one dimensional deblurring problem. Consider the true signal

$$\tilde{f} = (\cdots, f_{-m+1}, \cdots, f_0, f_1, \cdots, f_n, f_{n+1}, \cdots, f_{n+m}, \cdots)^t. \tag{2.1}$$

and the blurring function given by

$$h = (\cdots, 0, 0, h_{-m}, h_{-m+1}, \cdots, h_0, \cdots, h_{m-1}, h_m, 0, 0, \cdots)^t. \tag{2.2}$$

The blurred signal g is just computing the convolution of h and f, i.e., the i^{th} entry g_i of the blurred signal is given by

$$g_i = \sum_{j=-\infty}^{\infty} h_{i-j} f_j. \tag{2.3}$$

The deblurring problem is to reconstruct the signal $f = (f_1, f_2, \cdots, f_n)^t$ from blurring function h and a blurred signal $g = (g_1, g_2, \cdots, g_n)^t$ of finite length i.e.,

$$\begin{pmatrix} h_m & \cdots & h_0 & \cdots & h_{-m} & & & & \\ & h_m & & h_0 & & h_{-m} & & 0 & \\ & & \ddots & & \ddots & & \ddots & & \\ & & & \ddots & & \ddots & & \ddots & \\ & 0 & & & h_m & & h_0 & & h_{-m} \\ & & & & & h_m & \cdots & h_0 & \cdots & h_{-m} \end{pmatrix} \begin{pmatrix} f_{-m+1} \\ f_{-m+2} \\ \vdots \\ f_0 \\ f_1 \\ \vdots \\ f_n \\ f_{n+1} \\ \vdots \\ f_{n+m-1} \\ f_{n+m} \end{pmatrix} = \begin{pmatrix} g_1 \\ g_2 \\ \vdots \\ g_n \end{pmatrix}. \tag{2.4}$$

Thus the blurred signal g is determined not by f only, but also by $f_l = (f_{-m+1}, f_{-m+2}, \cdots, f_0)^t$ and $f_r = (f_{n+1}, f_{n+2}, \cdots, f_{n+m})^t$. Clearly, the above system is underdetermined. To overcome this, we set up certain assumptions called boundary conditions on the unknown data $f_{-m+1}, \cdots, f_0$ and $f_{n+1}, \cdots, f_{n+m}$ such that the number of unknowns equals the number of equations.

Let us we first rewrite (2.4) as

$$T_l f_l + T f + T_r f_r = g, \tag{2.5}$$

where

$$T_l = \begin{pmatrix} h_m & \cdots & h_1 \\ & \ddots & \vdots \\ & & h_m \\ & & \\ 0 & & \end{pmatrix}_{n\times m}, f_l = \begin{pmatrix} f_{-m+1} \\ f_{-m+2} \\ \vdots \\ f_{-1} \\ f_0 \end{pmatrix}_{m\times 1} \tag{2.6}$$

$$T = \begin{pmatrix} h_0 & \cdots & h_{-m} & & 0 \\ \vdots & \ddots & \ddots & \ddots & \\ h_m & \ddots & \ddots & \ddots & h_{-m} \\ & \ddots & \ddots & \ddots & \vdots \\ 0 & & h_m & \cdots & h_0 \end{pmatrix}_{n\times n}, f = \begin{pmatrix} f_1 \\ f_2 \\ \vdots \\ f_{n-1} \\ f_n \end{pmatrix}_{n\times 1} \tag{2.7}$$

$$T_r = \begin{pmatrix} & & 0 \\ & & \\ h_{-m} & & \\ \vdots & \ddots & \\ h_{-1} & \cdots & h_{-m} \end{pmatrix}_{n\times m}, f_r = \begin{pmatrix} f_{n+1} \\ f_{n+2} \\ \vdots \\ f_{n+m-1} \\ f_{n+m} \end{pmatrix}_{m\times 1}. \tag{2.8}$$

2.1 The Dirichlet boundary condition.

In the zero (or Dirichlet) boundary condition assumes that the values of f outside the domain of consideration are zero, i.e.,

$$f_l = f_r = 0,$$

the zero vector. The matrix system in (2.5) takes simplest form

$$Tf = g. \tag{2.9}$$

In (2.9) the coefficient matrix T is a Toeplitz matrix. In the two-dimensional case the resulting blurring matrices will be block-Toeplitz-Toeplitz-block (BTTB) matrices. FFTs can be used to impliment fast matrix vector multiplications for T.

2.2 Periodic boundary condition.

In the periodic boundary condition assumes that values of signal outside the domain of consideration is a repeat. i.e.,

$$f_j = f_{n-j}$$

for all j in (2.4) [1]. The matrix system in (2.5) becomes

$$Bf = [(0|T_l) + T + (T_r|0)]f = g, \tag{2.10}$$

where $(0|T_l)$ and $(T_r|0)$ are n-by-n Toeplitz matrices obtained by augmenting $(n - m)$ zero columns to T_l and T_r, respevtively.

In this case the coefficient matrix B is a circulant matrix. Hence B can be diagonalized by discrete Fourier matrix. In the two-dimensional case, the blurring matrix becomes block-circulant-circulant-block matrix which is diagonalized by two-dimensional FFTs (tensor product of one-dimensional FFTs).

2.3 Reflexive boundary condition.

In the Neumann boundary condition assumes the data outside of f are a reflection of the data inside f. This amounts to setting

$$\begin{array}{ccccccc} f_0 & = & f_1 & & f_{n+1} & = & f_n \\ \vdots & \vdots & \vdots & and & \vdots & \vdots & \vdots \\ f_{-m+1} & = & f_m & & f_{n+m} & = & f_{n-m+1} \end{array} \tag{2.11}$$

in (2.4). Thus (2.5) becomes

$$Af = [(0|T_l)J + T + (T_r|0)J]f = g, \tag{2.12}$$

where J is the n -by- n reversal matrix.

In (2.12) the coefficient matrix A is a Toeplitz-plus-Hankel matrix. In two-dimensional case the coefficient matrix is a block Toeplitz-plus-Hankel matrices with Toeplitz-plus-Hankel blocks which is diagonalized by the discrete cosine transform matrix provided that the blurring function h is symmetric.

The most important advantage of using Neumann boundary condition is that the solving a problem with Neumann boundary condition is twice as fast a solving a problem with the periodic boundary condition.

The solution f of (2.12) is given by

$$f = C\Lambda^{-1}C^T g, \tag{2.13}$$

where C is the discrete cosine transform matrix and Λ is the diagonal matrix holding the eigenvalues of A [9].

3 Background of mathematical transforms

3.1 Truncated Singular Value Decomposition

The deblurred image consists of two components : The first component is the exact image, and the second component is the inverted noise.

The inverted noise term can be gained using the singular value decomposition (SVD). The SVD of a blurring matrix A is defined as the decomposition

$$A = U\Sigma V^T, \tag{3.1}$$

$$A = \sum_{i=1}^{N} u_i \sigma_i v_i^T \tag{3.2}$$

Where U, V are orthogonal matrices and $\Sigma = diag(\sigma)$ is a diagonal matrix whose elements σ_i are non-negative and appear in non-increasing order,

$$\sigma_1 \geq \sigma_2 \geq \cdots \geq \sigma_N \geq 0$$

The quantities σ_i are called the singular values of A. The columns u_i of U are called the left singular vectors, while the columns v_i of V are the right singular vectors [10].

In this section we discuss the most important spectral filtering method called TSVD metthod [11]. For this method, we define the filter factors to be one for large singular values, and zero for the rest. More precisely,

$$\Phi_i = \begin{cases} 1 & i = 1, 2, \cdots, k \\ 0 & i = k+1, \cdots, N \end{cases}$$

The parameter k is called the truncation parameter or regularization parameter and it represents the number of SVD component maintained in the regularized solution where the k satisfies $1 \leq k \leq N$.

In SVD analysis the use of spectral filtering methods give us control-via the filter factors-over the spectral contents of the deblurred images. Spectral filtering methods work by choosing the filter factor ϕ_i in the computed solution,

$$f_{TSVD} = V\Sigma_{filt}^{-1} U^T g$$

where $\Sigma_{filt}^{-1} = \Phi\Sigma^{-1}$.

$$f_{TSVD} = \sum_{i=1}^{k} \phi_i \frac{u_i^T g}{\sigma_i} v_i \tag{3.3}$$

Note that as k increases, more terms are included in the SVD expansion, and consequently components with higher frequencies are included. Hence we can think of k as a way to control how much smoothing is introduced in the reconstruction. If some of the singular values in Σ are zero then A^{-1} not exists. We can avoid this unwanted situation by performing the computation only for non zero values of Σ, and setting all other Σ_{filt}^{-1} values to zero.

Generally blurring matrices are ill-conditioned and deblurring algorithms will be extremely sensitive to noise [1]. The ill-contitioning of the blurring matrices grow from the wide range of magnitudes of their eigenvalues [12]. Therefore redundant amplication of the noise at small eigenvalues can occur. Therefore choosing the regularization parameter for an ill-posed probllem is an art based on a combination of good heuristics and prior knowledge of the noise in the observations.

The norm of the spectral filtering solution in (3.3) becomes

$$\|f_{f_{TSVD}}\|_2^2 = \sum_{i=1}^{N} \left(\phi_i \frac{u_i^T g}{\sigma_i} \right)^2 \tag{3.4}$$

and the residual norm

$$\|g - Af_{TSVD}\|_2^2 = \sum_{i=1}^{N} \left((1-\phi_i) u_i^T g \right)^2. \tag{3.5}$$

For the TSVD method the norm of the solutioin $f_{TSVD} = f_k$ is a monotonically nondecreasing function of k, while the residual norm is monotonically nonincreasing.

Another complexity in regularization is the choice of k. Generalized cross-validation [13] is a technique that estimates k directly without requiring an estimate of the noise variance.

The best parameter for our spectral filtering method minimizes the GCV functional.

$$G(k) = \frac{||(I_N - AV\Phi\Sigma^{-1}U^T)g||_2^2}{(trace(I_N - AV\Phi\Sigma^{-1}U^T))^2} \tag{3.6}$$

The numerator is just $||(I_N - AV\Phi\Sigma^{-1}U^T)g||_2^2 = ||g - Af_{TSVD}||_2^2$, for which we already have a formula. We evaluate the denominator by noting that the trace of a matrix is the sum of its main diagonal elements, and the trace is invariant under orthogonal transformation, so

$$trace(I_N - AV\Phi\Sigma^{-1}U^T) = N - k$$

Which is easy to compute. So equation in (3.6) can be written in simpler form as

$$G(k) = \frac{||g - Af_{TSVD}||_2^2}{(N-k)^2}$$

$$G(k) = \frac{1}{(N-k)^2}\sum_{i=k+1}^{N}(u_i^T g)^2 \tag{3.7}$$

For best parameter choice is to minimize the GCV functional

$$t = arg\ minG(k) = arg\ min\frac{||g - Af_{TSVD}||_2^2}{(N-k)^2}, \tag{3.8}$$

where N is the number of pixels in the image, and

$$f_t = Vdiag(\frac{1}{\sigma_1}, \cdots, \frac{1}{\sigma_k}, 0, \cdots, 0)U^T g. \tag{3.9}$$

3.2 Discrete wavelet transform

A part of waveforms generate wavelets: the wavelet function and the scaling function. The wavelet function produces the wavelets, while the scaling function finds the approximate signal at that scale. The resulting wavelets include coarse-scale ones that have a long duration, and fine-scale ones that ones have a short amount of time.

Let $(f(1), f(2), \cdots, f(n))$ be a sample of a real signal $f(t)$. The wavelet transform express the signal as coefficients in a function space spanned by a set of basis functions. The basis of the wavelet transform consists of infinitely many scaled and shifted versions of a mother wavelet function[14]. The discrete wavelet transform (DWT) measures frequency at different time resolutions and locations. The signal is projected into the time-frequency plane. The basis functions are

$$\psi_{j,k} = 2^{j/2}\psi(2^j t - k) \tag{3.10}$$

Where ψ is the mother wavelet function. Any square integrable real function $f(t)$ can be represented in terms of this bases as

$$f(t) = \sum_{j,k} C_{j,k}\psi_{j,k}(t) \tag{3.11}$$

and the $C_{j,k} =< \psi_{j,k}(t), f(t) >$ are the coefficients of the DWT. A simple and commonly used wavelet is the Haar wavelet with the mother function

$$\psi_{Haar}(t) = \begin{cases} 1, & if \quad 0 \le t < 1/2 \\ -1, & if \quad 1/2 \le t < 1 \\ 0, & \quad otherwise \end{cases} \tag{3.12}$$

Discrete Haar wavelet transform has become an attractive domain for the deblurring of images due to its well matching behaviour with human visual system (HVS) and it is a system of filters that decomposes an input image into a set of four non-overlapping multiresolution sub-bands[15] denoted as LL (approximation sub-band), LH (Horizontal sub-band), HL (vertical sub-band) and HH (Diagonal sub-band). LH, HL and HH represents the finest scale wavelet coefficients and LL stands for the coarse-level coefficient. Due to its excellent spatial localization and multiresolution properties, the discrete wavelet transform is much applicable to analyzing image features such as edges or textured areas in the image[16]. The block matrix LL truncated by SVD method which makes image more clear and high PSNR value. The main advantage of using wavelet transform is to reconstruct deblurred image with very low truncation index k.

4 Proposed algorithm

X $\leftarrow$ Original image of size 512×512
B $\leftarrow$ Array containing blurred image of X.
P $\leftarrow$ Array containing point spread function; same size as B.
step 1: Without constructing blurring matrix, we compute eigen values of blurring matrix.
The eigen values of blurring matrix for periodic boundary condition is computed as

$$S = fft2(circshift(P, 1 - center)) \tag{4.1}$$

step 2: Eigen values of blurring matrix for Neumann boundary condition is computed as

$$S = dct2(dctshift(P, center))/dct(e_1), \tag{4.2}$$

where *dctshift* is a built-in Matlab function and e_1 is the first column of identity matrix.
step 3: We decompose original image X into four sub-bands by applying discrete Haar wavelet transform

$$i.e., [cA, cH, cV, cD] = dwt2(X,' haar'). \tag{4.3}$$

step 4: Construct blurred image B of X by using eigen vales of blurring matrix and coarse-scale dwt coefficients of X

$$i.e., B = real(ifft2(S. * fft2(cA))). \tag{4.4}$$

step 5: Arranging the eigen values of blurring matrix by decreasing order.
step 6: Use Generalization cross-validation to estimate k directly

$$i.e., G(k) = \frac{1}{(N-k)^2} \sum_{i=k+1}^{N} (u_i^T g)^2 \tag{4.5}$$

where $u_i^T g = fft2(B)$ and N is the number of pixels in the image.
step 7: Minimizing GCV functional tol=min G(k)
k is the truncation index and tol is the truncation tolerence that is any singular values less than tolerence is truncated.
step 8: Compute $A_k = VS^{-1}U^T B$
step 9: Finally, compute the deblurred image by applying inverse discrete Haar wavelet transform to A_k.

$$X_k = Idwt2(A_k, cH, cV, cD,' haar'). \tag{4.6}$$

5 Numerical experiments

This section provides the experimental results and analysis of the proposed scheme. This work is programmed in matlab 2016a with system specifications- windows 7 OS, intel i5 core processor and 64 bit operating system. figure 1 shows the original Barbara, Lena and Cameraman images of size $512 \times 512, 512 \times 512$ and 256×256 respectively. The Barbara, Lena and Cameraman images are blurred by the following two blurring functions [3].

(i) a Gaussian blur,

$$h_{ij} = \begin{cases} ce^{-0.1(i^2+j^2)} & if\ |i-j| \leq 8 \\ 0 & otherwise \end{cases}$$

(ii) an Out-of-focus blur,

$$h_{ij} = \begin{cases} c & if\ i^2+j^2 \leq 4 \\ 0 & otherwise \end{cases}$$

where c is the normalization constant such that $\sum_{i,j} h_{i,j} = 1$.

The noisy blurred Barbara, Lena and Cameraman images by Gaussian blur and Out-of-focus blur are shown in figure 2 and figure 3. Two boundary conditions are compared here: Periodic boundary condition and Neumann boundary condition. Relative error of the restored image is defined as $\frac{||f-f_t||_2}{||f||_2}$, where f is the original image and f_t is the restored image with regularization parameter t. In figure 4 to figure 7, we present the restored images with Gaussian and Out-of-focus blurring functions for the periodic and Neumann boundary conditions by TSVD method and images are reconstructed well with large number of truncation index k as shown in Table 1 and Table 2. From figure 8 to figure 11 are deblurred images reconstructed by DWT method for both periodic and Neumann boundary conditions with low truncation index k as shown in Table 3 and Table 4. The truncation tolerence, PSNR, relative error and truncation index are calculated both in TSVD and DWT method for Gaussian blur and Out-of focus blur as shown in Table 1 to Table 4. The restored images with periodic boundary conditions is showed in figure 4 to figure 11; one can easily see that the ringing effects appear at the boundary. We see that by imposing the Neumann boundary condition, the relative error and the ringing effect are the smallest. Also the Barbara and Lena images are better reconstructed by using the Neumann boundary condition than by using periodic boundary conditions.

(a) Barbara (b) Lena (c) Cameraman

Figure 1. Original images of (a) Barbara, (b) Lena and (c) Cameraman

(a) Barbara (b) Lena (c) Cameraman

Figure 2. Blurred images (a) Barbara, (b) Lena and (c) Cameraman by Gaussian blur

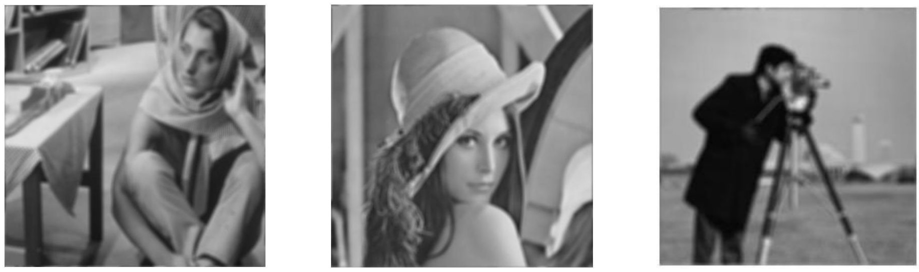

(a) Barbara (b) Lena (c) Cameraman

Figure 3. Blurred images (a) Barbara, (b) Lena and (c) Cameraman by Out-of-focus blur

(a) Barbara (b) Lena (c) Cameraman

Figure 4. Restoring (a), (b) and (c) by Gaussian blur with periodic boundary conditions using TSVD method.

(a) Barbara (b) Lena (c) Cameraman

Figure 5. Restoring (a), (b) and (c) by Gaussian blur with reflexive boundary conditions using TSVD method.

(a) Barbara (b) Lena (c) Cameraman

Figure 6. Restoring (a), (b) and (c) by Out-of-focus blur with periodic boundary conditions using TSVD method.

(a) Barbara (b) Lena (c) Cameraman

Figure 7. Restoring (a), (b) and (c) by Out-of-focus blur with reflexive boundary conditions using TSVD method.

(a) Barbara (b) Lena (c) Cameraman

Figure 8. Restoring (a), (b) and (c) by Gaussian blur with periodic boundary conditions using TSVD-DWT method.

(a) Barbara (b) Lena (c) Cameraman

Figure 9. Restoring (a), (b) and (c) by Gaussian blur with reflexive boundary conditions using TSVD-DWT method.

(a) Barbara (b) Lena (c) Cameraman

Figure 10. Restoring (a), (b) and (c) by Out-of-focus blur with periodic boundary conditions using TSVD-DWT method.

(a) Barbara (b) Lena (c) Cameraman

Figure 11. Restoring (a), (b) and (c) by Out-of-focus blur with reflexive boundary conditions using TSVD-DWT method.

Image	Blurring function	tolerence	PSNR	relative error	truncation index (k)
Barbara	Gaussian	1.67×10^{-8}	74.9536	0.0236	449
Lena	Gaussian	1.855×10^{-14}	89.11	0.0058	433
Cameraman	Gaussian	3×10^{-5}	74.53	00.0226	246
Barbara	Out-of-focus	0.0015	93.57	0.0027	510
Lena	Out-of-focus	0.0030	96.42	0.0023	508
Cameraman	Out-of-focus	0.0015	90.93	0.0057	254

Table 1. Summary of restoration results for periodic boundary condition by TSVD method.

Image	Blurring function	tolerence	PSNR	relative error	truncation index (k)
Barbara	Gaussian	1×10^{-4}	85.97	0.0112	338
Lena	Gaussian	0.0099	79.47	0.0112	417
Cameraman	Gaussian	3×10^{-4}	80.3580	0.0135	255
Barbara	Out-of-focus	0.0011	95.13	0.0034	511
Lena	Out-of-focus	0.0011	101.25	0.0011	511
Cameraman	Out-of-focus	0.0015	92.44	0.0051	255

Table 2. Summary of restoration results for Neumann boundary condition by TSVD method.

Image	Blurring function	tolerence	PSNR	relative error	truncation index (k)
Barbara	Gaussian	1.68×10^{-15}	78.46	0.0209	225
Lena	Gaussian	3.32×10^{-14}	85.42	0.0086	215
Cameraman	Gaussian	4.8×10^{-10}	76.34	0.0255	115
Barbara	Out-of-focus	0.0015	93.18	0.0051	254
Lena	Out-of-focus	0.0015	95.90	0.0032	254
Cameraman	Out-of-focus	0.0003	95.49	0.0042	126

Table 3. Summary of restoration results for periodic boundary condition by TSVD-DWT method.

Image	**Blurring function**	**tolerence**	**PSNR**	**relative error**	**truncation index** (k)
Barbara	Gaussian	3×10^{-4}	78.35	0.0188	209
Lena	Gaussian	3×10^{-4}	83.60	0.0105	195
Cameraman	Gaussian	2×10^{-5}	89.32	0.0156	101
Barbara	Out-of-focus	0.0015	94.52	0.0039	255
Lena	Out-of-focus	0.0015	98.13	0.0022	255
Cameraman	Out-of-focus	0.0015	90.85	0.0062	127

Table 4. Summary of restoration results for Neumann boundary condition by TSVD-DWT method.

6 Concluding remarks

In this paper, we have studied TSVD-based regularization method and DWT method for solving image restoration problems with periodic and Neumann boundary conditions for two different blurring functions. Numerical results suggest that TSVD method needs large number of truncation index to construct deblurred image while DWT method needs small number of truncation index. Advantage of the proposed algorithm to achieve best performance in relative error and truncation index without losing the quality of the image. For future work, proposed algorithm leads to different types of wavelet transform methods such as Daubechies, Coiflet to improvement in image deblurring and denoising techniques.

References

[1] R. C. Gonzalez and R. E. Woods, Digital image processing Reading, *MA: Addison-Wesley*, (1992).

[2] K. Castleman, Digital Image Processing, *Prentice-Hall, Englewood Cliffs, NJ*, 1996.

[3] A. K. Jain, Fundamentals of digital image processing, *Prentice-Hall, Inc.*, (1989).

[4] M. K. Ng, R. H. Chan and Wun-Cheung Tang, A fast algorithm for deblurring models with Neumann boundary conditions, *Journal on Scientific Computing, SIAM*, **21**, 851–866 (1999).

[5] H. C. Andrews, and Boby Ray Hunt, Digital image restoration, *Prentice-Hall*, (1977).

[6] I. Daubechies and G. Teschke, Variational image restoration by means of wavelets: Simultaneous decomposition, deblurring, and denoising, *Applied and Computational Hormonic Analysis, Elsevier*, **19**, 1–16 (2005).

[7] J. Kamm and J. G. Nagy, Kronecker product and SVD approximations image restorations, *Linear Algebra and its Applications, Elsevier*, **284**, 177–192 (1998).

[8] M. K. Ng, C. K. Cze and S. P. Yung, Wavelet Algorithms for Deblurring Models, *International Journal of Imaging Systems and Technology, Wiley Periodicals*, **14**, 113–121 (2004).

[9] K. R. Rao, and P. Yip, Discrete cosine transform: algorithms, advantages, applications, *Academic press*, (2014).

[10] G. H. Golub and C. F. Van Loan, Matrix computations, *Johns Hopkins Univ. press*, **3**, (2013).

[11] P. C. Hansen, J. G. Nagy and D. P. O'leary, Deblurring images: matrices, spectra, and filtering, *SIAM*, (2006).

[12] H. Werner Engl, M. Hanke and A. Neubauer, Regularization of inverse problems, *Springer Science & Business Media*, (1996).

[13] G. H. Golub, Michael Heath and Grace Wahba, Generalized cross-validation as a method for choosing a good ridge parameter, *Technometrics, Taylor & Francis Group*, **21**, 215–223 (1979).

[14] M. W. Frazier, An introduction to wavelets through linear algebra, *Springer Science & Business Media*, (2006).

[15] D. K. Ruch and Patrick J Van Fleet, Wavelet theory: an elementary approach with applications, *John Wiley & Sons*, (2011).

[16] P. Meerwald and A. Uhl, Survey of wavelet-domain watermarking algorithms. *Security and watermarking of multimedia contents III*, 505–516 (2001).

[17] S. Cheng, R. Liu, Y. He, X. Fan and Z. Luo, Blind image deblurring via hybrid deep priors modeling, *Neurocomputing, Elsevier*, **387**, 334–345 (2020).

[18] D. Zhang, Z. Liang and J. Shao, Joint image deblurring and super-resolution with attention dual supervised network, *Neurocomputing, Elsevier*, **412**, 187–196 (2020).

Author information

A. Padmanabha Reddy and K. Riyajuddin, Department of Studies in Mathematics Vijayanagara Sri Krishnadevaraya University, Ballari-583105, India.
E-mail: apreddy@vskub.ac.in and riyazuddin.k108@gmail.com

Received: March 28, 2021.
Accepted: July 24, 2021.